Mediterranean Journal of Hematology and Infectious Diseases

Original Article

Dynamic multiplex cytokine profiling to identify risk factors for Lung Consolidation and Necrotizing Transformation in Children with *Mycoplasma Pneumoniae* Pneumonia

Hailiang Yan[1] and Chuyi Zhang[1].

[1] Department of Pediatrics, Huizhou Zhongda Huiya Hospital, Huizhou, Guangdong 516081, China.

Competing interests: The authors declare no competing interest.

Abstract. ***Background*: Radiologic complications of pediatric *Mycoplasma pneumoniae* pneumonia (MPP), consolidation, and necrotizing pneumonia (NP) are difficult to anticipate early. We tested whether admission cytokines and short-term changes predict imaging outcomes.**
***Methods*: A retrospective cohort (Oct 2022–Sep 2024) of hospitalized children with PCR-confirmed MPP. Multiplex cytokines (including IL-6, IL-10, CXCL10/IP-10) were assayed from residual samples at admission (T0) and days 3–5 (T1). NP analyses were conditional on undergoing computed tomography (CT). Primary outcomes were WHO end-point CXR consolidation ≤14 days and CT-defined NP ≤28 days. Full-cohort 14-day CXR-consolidation risk (admission), post-T1 consolidation risk among event-free children (day 3–5 landmark), and 28-day NP risk conditional on being scanned. Penalized logistic models evaluated T0 and Δ(T0-T1) predictors among children event-free at T1, with AUC (bootstrap-corrected) and BH-FDR control.**
***Results*: Of 286 enrollments, 268 were analyzed; consolidation occurred in 96/268 (35.8%), CT was performed in 124/268 (46.3%), and identified NP in 28/124 (22.6%; 10.4% overall). In the Admission model, IL-6 (adjusted OR [aOR] 1.45, 95% CI 1.16–1.83; q=0.01), IP-10 (1.52, 1.21–1.93; q<0.01), and IL-10 (1.28, 1.03–1.60; q=0.04) predicted consolidation (AUC 0.78, 95% CI 0.73–0.83). In event-free children at T1 (n=180), ΔIL 6 (1.40, 1.12–1.76) and ΔIP 10 (1.48, 1.18–1.88) improved discrimination (AUC 0.84, 0.79–0.88). In CT-subset models, T0 IL-6 (1.67, 1.09–2.58) and ΔIL-6 (1.89, 1.22–3.00) were associated with NP (AUC 0.79). Findings were robust in prespecified sensitivity analyses.**
***Conclusions*: Admission cytokines and early rises, especially IL-6 and IP-10, enable pragmatic early risk stratification for consolidation, with ΔIL-6 also signaling NP risk in the CT-scanned subset. These results support external validation of a cytokine-based tool to inform imaging and triage.**

Keywords: *Mycoplasma pneumoniae*; Pediatrics; Cytokines; IL-6; IP-10; Necrotizing pneumonia; Consolidation; Prognostic modeling; Landmark analysis.

Citation: Yan H., Zhang C. Dynamic multiplex cytokine profiling to identify risk factors for lung consolidation and necrotizing transformation in children with *Mycoplasma pneumoniae* pneumonia. Mediterr J Hematol Infect Dis 2026, 18(1): e2026008, DOI: http://dx.doi.org/10.4084/MJHID.2026.008

Published: January 01, 2026 **Received: October 26, 2025** **Accepted: December 09, 2025**

Correspondence to: Hailiang Yan. 186 Zhongxing North Road, Dayawan District, Huizhou, Guangdong 516081, China. E-mail: yanhailiang0a@163.com

Introduction. Severe radiologic complications of pediatric *Mycoplasma pneumoniae* pneumonia (MPP), such as lung consolidation and necrotizing pneumonia (NP), present significant clinical challenges due to the difficulty in early prediction and diagnosis. The current literature highlights the role of immune dysregulation and various biomarkers in anticipating these severe outcomes. Studies have identified several risk factors and biomarkers that could potentially aid in early prediction. Elevated levels of inflammatory markers such as C-reactive protein (CRP), lactate dehydrogenase (LDH), and interleukin-6 (IL-6) have been associated with severe MPP and NP.[1-3] Additionally, factors such as prolonged fever duration, elevated D-dimer levels, and specific cytokine profiles, including decreased IL17A levels, have been linked to severe MPP and NP.[4-6] Nomogram models incorporating these biomarkers, along with clinical features like age and respiratory symptoms, have been developed to predict the severity of MPP.[7,8] Furthermore, distinguishing *Mycoplasma pneumoniae* necrotizing pneumonia from bacterial necrotizing pneumonia (BNP) can be aided by specific biomarkers, such as white blood cell count, procalcitonin, and pleural fluid characteristics.[9] Despite these advancements, there remains an unmet need for dynamic biomarkers that can reliably predict severe radiologic outcomes early in the hospitalization process.[1,10]

Although single-timepoint cytokine studies in pediatric *Mycoplasma pneumoniae* pneumonia (MPP) show that IL-6/IL-10 and CXCL10/IP-10 correlate with clinical severity,[11,12] most investigations are cross-sectional and rely on routine radiology reports rather than on centrally, blindly adjudicated imaging outcomes aligned with standardized WHO endpoints.[13] Risk tools for necrotizing complications likewise emphasize static clinical or laboratory features and large-lesion radiography without standardized adjudication.[14] By contrast, outside MPP, serial cytokine trajectories demonstrate prognostic value in pediatric acute respiratory failure.[15] These gaps motivate the evaluation of whether baseline levels and early changes in key cytokines improve the prediction of centrally adjudicated CXR-defined consolidation (14 days) and CT-defined necrotizing pneumonia (28 days) in children.

We aimed to determine whether baseline (T0) cytokine levels and short-term changes (ΔT0-T1) associate with radiologic complications in pediatric Mycoplasma pneumoniae pneumonia, specifically CXR-defined consolidation within 14 days and CT-defined necrotizing pneumonia within 28 days. To address this objective, we conducted a retrospective single-center cohort study of hospitalized, PCR-confirmed cases and quantified a multiplex cytokine panel (IL-6, IL-8, IL-10, IL-17A, IFN-γ, TNF-α, and CXCL10/IP-10) using residual clinical specimens collected at four prespecified time points (T0–T3). Analyses incorporated an explicit day-3 landmark at T1, restricting Δ-based predictors to participants who remained event-free at that time to mitigate immortal-time bias and preserve temporal ordering between biomarkers and outcomes.

Methods.

Study design and participants. We conducted a retrospective, single-center, non-interventional cohort of hospitalized children with PCR-confirmed MPP at Huizhou Zhongda Hulya Hospital from October 2022 to September 2024. This study was conducted in accordance with the Declaration of Helsinki. The protocol was reviewed and approved by the Ethics Committee of Huizhou Zhongda Hulya Hospital, which waived the requirement for informed consent because the study was a retrospective analysis of de-identified, routinely collected data and posed minimal risk to participants. All data were anonymized prior to analysis.

Eligible participants were hospitalized children aged 1 month to 16 years with PCR-confirmed *Mycoplasma pneumoniae* pneumonia during October 2022 to September 2024. Inclusion required availability of a residual clinically indicated blood sample within 24 hours of admission (T0) for cytokine measurement and follow-up through 28 days to allow blinded adjudication of CXR-defined consolidation ≤14 days and CT-defined necrotizing pneumonia ≤28 days (CT obtained at clinicians' discretion). We excluded screen failures identified prior to analysis: inability to verify PCR positivity; absence of a T0 residual sample within 24 hours; insufficient clinical or imaging data for outcome adjudication within the prespecified windows; age outside the 1-month–16 years range; or not hospitalized for the index episode. Co-infections, pre-T0 systemic steroids, macrolide-resistance status, and chronic comorbidities were not exclusionary and were recorded for sensitivity analyses or covariate assessment.

Cytokine sampling and measurements. The hospital clinical laboratory processed venous blood collected for routine care. Serum or plasma was separated by standard centrifugation and aliquoted, and study aliquots were cryopreserved at −80 °C. For testing, aliquots were thawed once on ice, gently mixed, and clarified by brief centrifugation. Repeat freeze–thaw cycles were avoided.

Assay platform, reagents, and core operating parameters: Cytokines were quantified using a multiplex bead-based immunoassay (Luminex® xMAP®): MILLIPLEX® MAP Human Cytokine/Chemokine Magnetic Bead Panel, HCYTMAG-60K (Merck Millipore Sigma, Burlington, MA, USA), run according to the manufacturer's instructions on a Luminex platform with standard acquisition software. After a single controlled thaw on ice, 25 µL serum/plasma per well was combined with antibody-immobilized magnetic beads and incubated 2 hours at room temperature (20–25 °C)

with shaking (the IFU also permits overnight, 16–18 h at 4 °C). Plates were then washed and incubated with detection antibodies for 1 hour at room temperature, followed by streptavidin–phycoerythrin for 30 minutes at room temperature, with washes between steps. Calibration used six-point standards spanning 3.2–10,000 pg/mL and five-parameter logistic (5-PL) curve-fitting. Concentrations were exported in pg/mL for analysis. Per kit specifications, the lower limits of detection for our analytes were: IL-6 1.3 pg/mL; IL-8 0.7 pg/mL; IL-10 1.6 pg/mL; IL-17A 1.2 pg/mL; IFN-γ 1.1 pg/mL; TNF-α 1.1 pg/mL; and CXCL10/IP-10 14.0 pg/mL; the upper reportable limit was the highest standard, 10,000 pg/mL, with above-range samples diluted and re-assayed when available.

Cytokines were measured from residual serum or plasma at four prespecified windows: T0 within 24 hours of admission, T1 on days 3–5, T2 on days 7–10, and T3 within 48 hours before discharge. Because the median length of stay was <7 days, T2 sampling was permitted at hospital-affiliated outpatient sites. Accordingly, the T2 subset may overrepresent children who either improved sufficiently to return on time or remained hospitalized due to greater severity; T2 measures were therefore summarized descriptively and were not used in the primary multivariable models, which relied on T0/T1. Concentrations were log2-transformed prior to analysis, and Δ values were defined as log2 fold-changes from T0 to T1. To avoid bias from incomplete sampling, Δ predictors were computed only when both T0 and T1 were available. For consolidation, we used Δ predictors exclusively within the day-3 landmark set, and for NP (CT subset), we allowed Δ predictors only when the T1 sample predated the first CT diagnosing NP (temporal alignment verified for all NP events included in modeling). Models used complete cases for their specified predictors; no imputation was performed.

Sampling completeness and attrition categories: Sampling completeness declined at later windows. To document reasons for missed draws, we classified non-collection into prespecified, non-mutually-exclusive categories recorded from the chart and laboratory logs: (i) early discharge before the window; (ii) outpatient scheduling/no-show after discharge (T2); (iii) transfer to another facility or higher-level care; (iv) insufficient specimen volume or sample rejection; and (v) operational/logistic constraints.

Because Δ predictors reflect change up to T1, we retrospectively abstracted systemic corticosteroid exposure from the medication administration record (MAR) to identify new initiation or dose intensification occurring after T0 and before T1. Intensification was defined a priori as either an increase in prednisone-equivalent daily dose by ≥0.5 mg/kg/day or initiation of pulse-dose methylprednisolone. We coded a single indicator (SteroidChange_T0-T1: none vs initiated/intensified) and, when data permitted, a three-level variable (none; continued from pre-T0 without intensification; initiated/intensified).

Outcomes and imaging adjudication. Primary outcomes were chest radiograph (CXR)–defined consolidation within 14 days of admission, using the World Health Organization end-point definition, and computed-tomography (CT)–defined NP within 28 days. Imaging was obtained at the clinicians' discretion and was centrally, blindly adjudicated according to prespecified criteria without access to cytokines or other predictors. Accordingly, the NP component estimates risk among scanned children (a conditional evaluation) and is not extrapolated to unscanned children. All participants underwent CXR. A subset underwent CT based on clinical indications. Incidence and confidence intervals for imaging and outcomes are reported with explicit denominators to promote transparency.

CT was performed at the clinicians' discretion; therefore, NP models were restricted to the CT subset and should be interpreted conditionally on the presence of CT. The primary NP analysis used Firth-penalized logistic regression with predictors limited to T0 IL-6 and, when temporally valid, ΔIL-6 (T1 prior to the first CT establishing NP). To probe selection on observed covariates into the scanned subset, we conducted a pre-specified sensitivity analysis using inverse-probability-of-scanning weights (IPSW) estimated via logistic regression for the probability of receiving CT within 28 days as a function of baseline variables available before CT (age, sex, pre-T0 systemic steroids, viral coinfection, and T0 cytokines IL-6, IL-10, and CXCL10/IP-10). Stabilized weights were truncated at the 1st/99th percentiles to curb extreme values, and robust (sandwich) standard errors were used. Because Firth penalization is not standard with probability weights, the IPSW sensitivity used weighted logistic regression with the same predictors, interpreted alongside the primary Firth model. We did not fit a Heckman two-stage model because we lacked a credible exclusion-restriction variable that affects scanning but not NP risk. Instead, we report the IPSW sensitivity and make the target evaluation explicit (risk among children who are scanned). The NP component's generalizability is therefore limited to settings with similar CT-ordering practices.

Statistical analysis. We summarized continuous variables as medians (IQRs) and categorical variables as counts with 1 decimal place. Key proportions are reported with

Wilson 95% confidence intervals (CIs). Cytokines were analyzed on the log2 scale. Δ predictors were defined as log2 fold-change from T0 to T1. Univariable screening used logistic regression for each cytokine with

Benjamini–Hochberg false-discovery rate (FDR) control within outcome families. Multivariable inference used penalized logistic regression tailored to each decision point: an Admission model incorporating T0 cytokines to predict CXR-defined consolidation ≤14 days in the full cohort, and a day-3 landmark model restricted to participants event-free at T1 using Δ cytokines (T0-T1) to predict post-T1 consolidation. For NP in the CT subset, we used Firth-penalized logistic regression with predictors T0 IL-6 and, when temporally valid, ΔIL-6. Temporal validity was defined as a priori as the T1 sample collected strictly before the first CT that established NP. All primary multivariable models were cytokine-only and are therefore interpreted as mutually adjusted across cytokines.

To assess robustness to confounding while limiting overfitting, we pre-specified sensitivity models that added age, sex, viral coinfection, and pre-T0 systemic steroids. Because Δ predictors can be influenced by intercurrent therapy, we specifically addressed steroid initiation/intensification between T0 and T1 using three complementary approaches in the landmark analysis: adding a SteroidChange_T0-T1 indicator as a covariate, inverse-probability-of-treatment weighting (IPTW) for starting/intensifying steroids before T1 with stabilized weights from baseline covariates (age, sex, viral coinfection, pre-T0 steroids, and T0 IL-6, IL-10, CXCL10/IP-10), truncating at the 1st/99th percentiles and using robust standard errors, and restriction to children without steroid change before T1. For NP, because CT was obtained at the clinician's discretion, the primary evaluation is conditional on scanning. We added inverse-probability-of-scanning sensitivity using stabilized, truncated weights from baseline covariates, with robust standard errors, and interpreted alongside the Firth model.

Model performance was evaluated by discrimination and calibration. Clinical utility was examined using decision curve analysis (DCA) across 5–40% thresholds, a range chosen a priori to reflect feasible decision points for early imaging/consult escalation in this population (lower thresholds imply imaging nearly all children; higher thresholds exceed the cohort prevalence). For each threshold *pt*, the net benefit was calculated as, and we also reported the net reduction in interventions per 100 versus treating-all. Uncertainty in the model curve was summarized using pointwise 95% bootstrap bands (patient-level resampling with refitting); treat-all and treat-none are deterministic and shown without bands.

Results. Out of 286 hospitalized children with PCR-confirmed Mycoplasma pneumoniae pneumonia, 268 were included after a quality review of the data (Figure 1). The median age was 6.1 years (IQR 3.2–9.4), 53.0% were male, and the median length of stay was 6 days (IQR 4–9). Sampling occurred within predefined windows: T0 for all 268 children (100.0%), T1 for 212 children (79.1%), T2 for 148 children (55.2%; with 41.2% inpatient and 58.8% outpatient), and T3 for 96 children (35.8%). Before T0, 30 children (11.2%) received systemic steroids, and 64 (23.9%) had a viral coinfection. Macrolide-resistance testing was available for 152 children (56.7%), with resistance found in 44 (28.9%). All children had chest radiography, with 96 (35.8%) meeting the WHO endpoint for consolidation within 14 days. Computed tomography was performed on 124 children (46.3%), identifying necrotizing pneumonia (NP) in 28 children (22.6%; 10.4% overall) (**Tables 1–2** and **Figure 1**).

Table 1. Baseline characteristics and sampling availability.

Characteristic	Value
Age (years) median (IQR)	6.1 (3.2–9.4)
Male, n (%)	142 (53.0%)
Length of stay (days), median (IQR)	6 (4–9)
Pre-T0 systemic steroids, n (%)	30 (11.2%)
Viral coinfection, n (%)	64 (23.9%)
Macrolide-resistance genotype tested, n (%)	152 (56.7%)
Macrolide-resistant among those tested, n/N (%)	44/152 (28.9%)
Cytokine sampling windows	
T0 (≤24 h from admission), n (%)	268 (100.0%)
T1 (day 3–5), n (%)	212 (79.1%)
T2 (day 7–10), n (%)	148 (55.2%)
inpatient T2 draws, n/N (%)	61/148 (41.2%)
outpatient T2 draws, n/N (%)	87/148 (58.8%)
T3 (≤48 h pre-discharge), n (%)	96 (35.8%)
Landmark set (event-free at T1), n/N (%)	180/212 (84.9%)

A comparison of baseline characteristics between scanned and unscanned children (age, sex, pre-T0 steroids, viral coinfection, and T0 IL-6/IL-10/IP-10) was summarized using absolute standardized differences to assess selection bias into the CT subset (**Supplementary Table S1A**). Attrition rates were 20.9% at T1, 44.8% at T2, and 64.2% at T3. **Supplementary Table S1B** details reasons for missing data at each window, while **Supplementary Table S1C** compares baseline characteristics (age, sex, pre-T0 steroids, viral co-infection, and T0 cytokines) between children with and without samples at T1/T2/T3 to evaluate selection bias. Given these patterns, findings from T2 and T3 are interpreted descriptively, with primary analyses focused on T0 and T1.

In the cytokine-only multivariable model (mutually adjusted across cytokines), higher admission IL-6, CXCL10/IP-10, and IL-10 predicted CXR-defined consolidation with mutually adjusted ORs per log2 unit of 1.45 (95% CI 1.16–1.83; q=0.010), 1.52 (1.21–1.93; q<0.010), and 1.28 (1.03–1.60; q=0.040), respectively.

Table 2. Imaging and outcome incidence with 95% Cis.

Outcome	n/N (%)	95% CI (Wilson)
CXR-defined consolidation within 14 days	96/268 (35.8%)	30.3–41.7%
CT obtained within 28 days	124/268 (46.3%)	40.4–52.2%
Necrotizing pneumonia among CT-scanned	28/124 (22.6%)	16.1–30.7%
Necrotizing pneumonia in full cohort	28/268 (10.4%)	7.3–14.7%

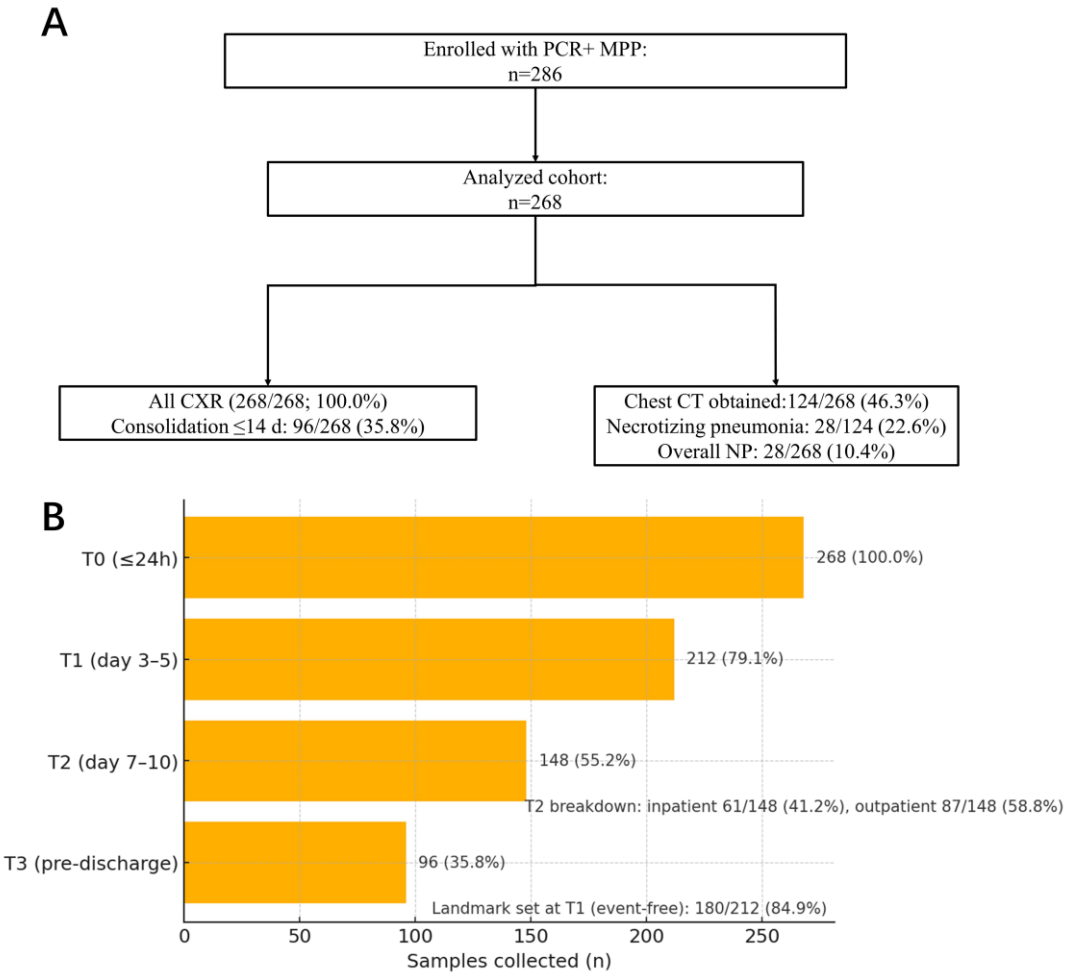

Figure 1. Cohort flow and sampling timeline. A) Diagram of 286 children enrolled with MMP, 268 participants were analyzed, universal CXR with 96/268 (35.8%) meeting WHO end-point consolidation within 14 days, and CT obtained in 124/268 (46.3%) with NP in 28/124. **B**) Sampling completeness at prespecified windows using residual clinical specimens.

Discrimination was AUC 0.78 (95% CI 0.73–0.83; optimism-corrected 0.76) and calibration slope 0.97. Results were similar after adding age, sex, viral coinfection, and pre-T0 steroids, supporting the primary cytokine-only specification (**Table 3**, **Figure 2**, and **Supplementary Table S2**).

Among children event-free at T1 (n=180/212; post-T1 events=54), rises in IL-6 and CXCL10/IP-10 were associated with subsequent consolidation (mutually adjusted ORs per log2 fold-change 1.40 [95% CI 1.12–1.76; q=0.004] and 1.48 [1.18–1.88; q=0.002]). Discrimination improved versus admission (AUC 0.84, 95% CI 0.79–0.88; optimism-corrected 0.82) with a calibration slope of 1.02. Decision-curve analysis (5–40% thresholds) showed higher net benefit than treat-all/none, with bootstrap 95% confidence bands and illustrative gains at sentinel thresholds: at 10%, model NB 0.228 versus treat-all 0.222 (≈5.5 fewer interventions per 100); at 20%, 0.153 versus 0.125 (≈11.3 fewer/100), at 30%, 0.017 versus 0.000 (≈3.9 fewer/100), and at 40%, model NB 0.001 while treat-all was harmful (−0.167; ≈25.2 fewer/100). Because Δ predictors may be influenced by therapy, we examined intercurrent steroid initiation/intensification before T1: covariate adjustment, IPTW using baseline covariates, and restriction to children without steroid change. These approaches yielded estimates and performance similar to the primary model (**Table 3**, **Figure 3**, and **Supplementary Table S2**).

In children who underwent CT (n=124; NP=28), Firth-penalized models (cytokine-only, mutually adjusted) associated higher T0 IL-6 and rising IL-6 with

Table 3. Multivariable models and performance.

Admission model (T0) for radiographic consolidation			
Predictor	**Mutually adjusted OR across cytokines (95% CI)**	***p* (Wald)**	**FDR q**
IL-6 (baseline)	1.45 (1.16–1.83)	0.0014	0.010
CXCL10/IP-10 (baseline)	1.52 (1.21–1.93)	0.0004	<0.010
IL-10 (baseline)	1.28 (1.03–1.60)	0.0280	0.040
Day-3 landmark model (event-free at T1; N=180; post-T1 events = 54)			
ΔIL-6	1.40 (1.12–1.76)	0.0035	0.004
ΔCXCL10/IP-10	1.48 (1.18–1.88)	0.0010	0.002
NP exploratory model (CT subset; N=124; NP events = 28; Firth-penalized)			
IL-6 (baseline)	1.67 (1.09–2.58)	0.0196	0.020
ΔIL-6 (T0-T1)	1.89 (1.22–3.00)	0.0056	0.011

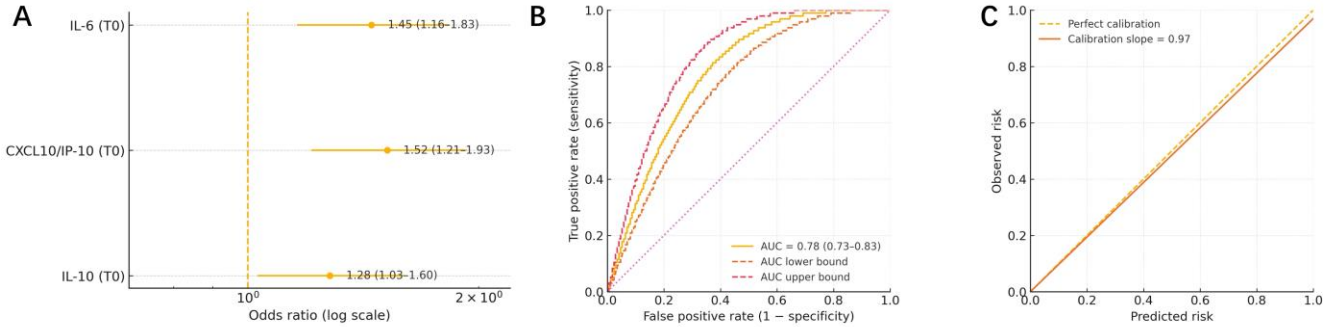

Figure 2. Admission model for predicting CXR-defined consolidation. Penalized multivariable logistic regression using baseline (T0) cytokines in the full cohort (N = 268; events = 96). **A**), Adjusted ORs per $\log_2$ unit with 95% CIs on a log scale: IL-6 1.45 (95% CI 1.16–1.83), CXCL10/IP-10 1.52 (1.21–1.93), IL-10 1.28 (1.03–1.60). Wald *p-values and Benjamini–Hochberg FDR q-values* correspond to Table 3. **B**), Apparent AUC 0.78 (95% CI 0.73–0.83) and optimism-corrected AUC 0.76 (0.632+ bootstrap). **C**) Calibration slope 0.97 with decile-based observed risks. Vertical dashed line denotes OR = 1.0; error bars represent 95% CIs.

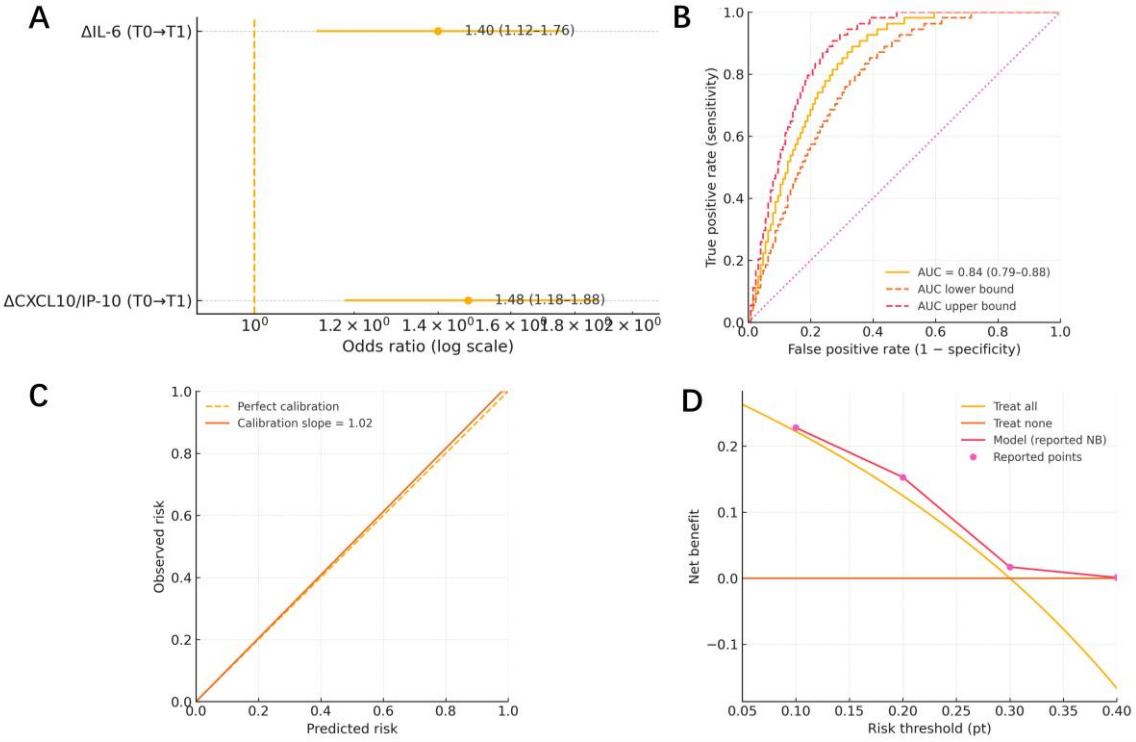

Figure 3. Day-3 landmark model for predicting subsequent consolidation. Landmark analysis restricted to participants event-free at T1 (N = 180/212; post-T1 events = 54). **A**), Δ predictors are $\log_2$ fold-changes from T0 to T1: ΔIL-6 aOR 1.40 (95% CI 1.12–1.76) and ΔCXCL10/IP-10 aOR 1.48 (1.18–1.88) with Wald *p* values and BH-FDR q values as in Table 3. **B**), AUC 0.84 (95% CI 0.79–0.88) with optimism-corrected AUC 0.82. **C**), Calibration slope 1.02. **D**), Net-benefit curves showing the landmark model outperforming treat-all and treat-none for thresholds ≈5–40% (event rate ≈30%). Vertical dashed line in (A) marks OR = 1.0; error bars denote 95% CIs.

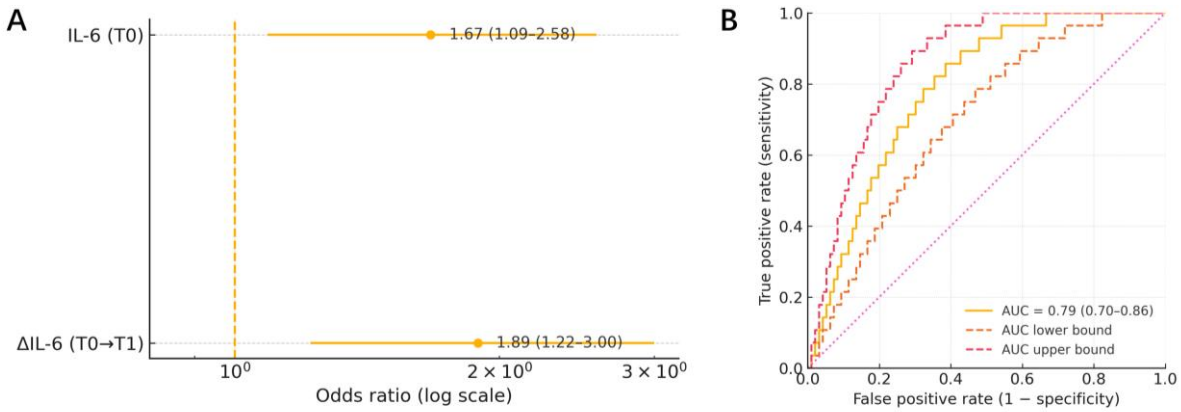

Figure 4. Exploratory models for CT-defined necrotizing pneumonia (CT subset). Firth-penalized logistic regression among children with CT (N = 124; NP events = 28). ***Panel A (Forest plot):*** Higher admission IL-6 and rising IL-6 from T0→T1 associate with NP—T0 IL-6 aOR 1.67 (95% CI 1.09–2.58) and ΔIL-6 aOR 1.89 (1.22–3.00)—with ORs per log2 unit and 95% CIs (Wald). ***Panel B (ROC):*** Apparent AUC 0.79 with optimism-corrected AUC 0.77 (bootstrap 95% CI 0.70–0.86). Vertical dashed line in Panel A marks OR = 1.0; error bars denote 95% Cis.

NP (OR 1.67, 95% CI 1.09–2.58; and 1.89, 1.22–3.00), with AUC 0.79 (optimism-corrected 0.77). In the CT subset (n = 124), 98 (79.0%) had T1 collected before the first CT and were included in ΔIL-6 analyses, including 22/28 (78.6%) NP cases; 26 were excluded (no T1, n = 16; T1 after CT, n = 8; unverifiable timing, n = 2). To probe selection into scanning, inverse probability of scanning weighting based on baseline covariates yielded directionally consistent associations and similar discrimination. By design, these NP estimates are conditional on being scanned and are not extrapolated to unscanned children. IPSW sensitivity produced directionally consistent forecasts (**Table 3**, **Figure 4**, and **Supplementary Table S2**).

Across prespecified checks (**Supplementary Table S2**), effect sizes, discrimination, and calibration were stable. For the admission model, adding clinical covariates, excluding pre-T0 steroids, removing viral coinfections, or adjusting for macrolide resistance produced AUCs of 0.77–0.79 (corrected 0.75–0.77) and slopes of 0.96–0.98, with IL-6 and CXCL10/IP-10 remaining significant. At the same time, IL-10 attenuated to borderline significance in the resistance subset. For the landmark models, handling steroid initiation/intensification between T0 and T1 by covariate adjustment, IPTW, or restriction left ΔIL-6 and ΔCXCL10/IP-10 materially unchanged (OR ranges 1.36–1.39 and 1.45–1.47) with AUC 0.83–0.84 (corrected 0.81–0.82) and slopes ≈1.01–1.02. In NP analyses, adding clinical covariates, removing coinfections, or applying scanning weights yielded IL-6 (T0) OR 1.59–1.66 and ΔIL-6 OR 1.81–1.89 with apparent AUC 0.78–0.79 (corrected 0.76–0.77 for unweighted Firth models), reinforcing robustness while acknowledging conditional transportability (**Supplementary Table S2**).

Calibration-in-the-large (intercept) is reported alongside slope in **Figures 2–4** and **Supplementary Table S1**, and a simple risk-stratification table showing bins at 10%, 20%, 30% with observed event rates is provided in **Supplementary Table S3** to support pathway thresholding.

Discussion. In this retrospective cohort of hospitalized children with MMP, we found that both admission cytokines and early rises (days 3–5) provided clinically meaningful, temporally coherent predictions of adjudicated CXR-defined consolidation, and ΔIL-6 signaled NP risk among scanned children. These results justify a pragmatic, adjunctive, cytokine-anchored pathway focused on the T0/T1 windows, with NP findings interpreted conditionally on scanning.

We make our target evaluation explicit and delimit where they transport: (i) 14-day CXR-defined consolidation risk at admission in the full hospitalized MPP cohort; (ii) post-T1 (day 3–5) consolidation risk among children event-free at T1; and (iii) 28-day CT-defined NP risk among children who underwent CT, an explicitly conditional estimate that transports only to scanned children and to centers with similar CT-ordering practices.[16-18] In our data, discrimination was AUC 0.78 (bootstrap-corrected 0.76) at admission and AUC 0.84 (corrected 0.82) at day-3. In the CT subset, the NP model had an AUC of 0.79 (corrected to 0.77). Adding a minimal clinical panel (age, sex, viral co-infection, pre-T0 steroids) changed AUC trivially (Admission 0.78 vs 0.79; Landmark 0.84 vs 0.84; NP 0.79 vs 0.78), aligning with literature that cytokines (IL-6, CXCL10/IP-10, IL-10) carry the most discriminative signal in pediatric CAP/MPP. That decision-curve net benefit, not tiny AUC deltas, should guide adoption.[19-23] We report calibration-in-the-large alongside slope and provide simple risk strata (<10%, 10–<20%, 20–<30%, ≥30%) to support local thresholding and safety monitoring.[16,19]

We outline a research phase, adjunctive protocol using T0 (≤24 h) and T1 (day 3–5) cytokines with center-

calibrated operating points (defaults <10% low, ≥20% high within a 5–40% decision curve range) and a pragmatic Δ trigger ≥ +1.0 log2: de-prioritize CT when risk is low, and Δ is stable or declining. Escalate imaging/consultation when risk is high, or Δ rises, always under clinician override.[18,19] Because CT is clinician-directed, NP findings depend on scanning and are likely to reflect unmeasured drivers (clinical trajectory, oxygen need/SaO2, auscultation/respiratory distress, worsening or large lesion CXR, pleural concern, prior consults, operational constraints).[18,24] To preserve chronological order, ΔIL 6 was analyzed only when T1 preceded the first CT. Later windows were non-random, so T2/T3 summaries are descriptive. Safeguards — single-thaw multiplex pre-analytics, Firth penalization for small NP events, 0.632+ optimism correction, and TRIPOD-aligned reporting — support internal validity while keeping Δ effects associative.[16,25-27]

Immune maturation suggests IL-6 may be less specific in infants (<3 y), whereas CXCL10/IP-10 may provide a more stable signal in school-age children (≥3 y). Accordingly, we recommend age-aware calibration of the same 10%/20% operating points and focusing Δ-based triggers at day-3–5.[11,22,23] Therapeutics can modulate cytokines, macrolides are immunomodulatory, and IVIG can lower inflammatory mediators, so Δ associations remain prognostic. Global macrolide resistance in *Mycoplasma pneumoniae* argues for thoughtful escalation within an adjunctive strategy.[28,29] Feasibility depends on platform and logistics: on-site Luminex/multiplex with daily batching can deliver same-day/next-day turnaround, whereas send-out testing often exceeds 24 h. A limited panel (IL-6, IP-10 ± IL-10) with verified LoD/LoQ and inter-assay CV ≤15–20% can lower barriers to adoption.[25] Generalizability remains restricted: NP results transport only to scanned children, and overall performance depends on center-specific CT thresholds and workflows. Therefore, external, multi-site validation with local calibration is required before broader use.[16-18]

This single-center, retrospective study is susceptible to design and data constraints that temper inference. NP was evaluated only among children who underwent CT, introducing spectrum and selection considerations. Δ-cytokine models apply only to children who are event-free at T1, and later windows were non-random because of discharge timing and outpatient follow-up. The residual-sample design contributed to missingness, and unmeasured confounding may persist. We mitigated risks using Firth penalization, optimism correction, inverse probability weighting for scanning, steroid-change controls, and TRIPOD-aligned transparent reporting, but these safeguards do not substitute for external validation.

Next steps are external, multi-site validation with center-specific calibration of operating points, including age-aware thresholds (<3 y vs ≥3 y) and deployment of a limited IL-6-6/IP-IP-10 (± IL-10) panel. We propose a prospective pathway evaluation with safety monitoring and an impact study on CT utilization, clinical outcomes, and workflow. In the interim, our findings support the pragmatic, adjunctive use of T0/T1 cytokines to inform early triage and targeted imaging, while keeping NP inferences conditional on being scanned.

Ethics approval and consent to participate. This study was conducted in accordance with the Declaration of Helsinki. The protocol was reviewed and approved by the Ethics Committee of Huizhou Zhongda Huiya Hospital, which waived the requirement for informed consent because this was a retrospective analysis of de-identified routinely collected data and posed no more than minimal risk to participants. All data were anonymized prior to analysis.

Data availability statement. Data sets generated during the current study are available from the corresponding author on reasonable request.

Author Contribution Statement. The authors confirm contribution to the paper as follows: study conception and design: H.Y.; data collection: H.Y., C.Z.; analysis and interpretation of results: H.Y., C.Z.; draft manuscript preparation: H.Y., C.Z. All authors reviewed the results and approved the final version of the manuscript.

References:

1. Zhang, X., Sun, R., Jia, W., Li, P., & Song, C. (2024). Clinical Characteristics of Lung Consolidation with Mycoplasma pneumoniae Pneumonia and Risk Factors for Mycoplasma pneumoniae Necrotizing Pneumonia in Children. Infectious Disease and Therapy, 1-15. https://doi.org/10.1007/s40121-023-00914-x PMid:38265626 PMCid:PMC10904708
2. Wang, L., Hu, Z., Jiang, J., & Jin, J. (2024). Serum inflammatory markers in children with Mycoplasma pneumoniae pneumonia and their predictive value for mycoplasma severity. World Journal of Clinical Cases, 12(22), 4940-4946. https://doi.org/10.12998/wjcc.v12.i22.4940 PMid:39109035 PMCid:PMC11238786
3. Zhang, Y. X., Li, Y., Wang, Y., Ren, Y. F., Yang, Y., Qi, J., Yang, H., Liang, X., & Zhang, R. F. (2024). Prospective cohort study on the clinical significance of interferon-γ, D-dimer, LDH, and CRP tests in children with severe mycoplasma pneumonia. Medicine, 103(41), e39665. https://doi.org/10.1097/MD.0000000000039665 PMid:39465799 PMCid:PMC11479529
4. Zhou, Y., Hu, M., Ye, B., Chen, Z., & Zhang, Y. (2020). Early prediction of necrotizing pneumonia from mycoplasma pneumoniae pneumonia with large pulmonary lesions in children. Scientific Reports, 10(1), 19061. https://doi.org/10.1038/s41598-020-76083-5 PMid:33149220 PMCid:PMC7643079
5. Yang, M., Meng, F., Wang, K., Gao, M., Lu, R., Li, M., Zhao, F., Huang, L., Zhang, Y., Cheng, G., Cheng, G., & Wang, X. (2017). Interleukin 17A as a good predictor of the severity of Mycoplasma pneumoniae pneumonia in children. Scientific Reports, 7(1), 12934. https://doi.org/10.1038/s41598-017-13292-5 PMid:29021577 PMCid:PMC5636901
6. Luo, X. qin, Luo, J., Wang, C. jie, Luo, Z., Tian, D., & Xie, X. hong.

(2023). Clinical features of severe Mycoplasma pneumoniae pneumonia with pulmonary complications in childhood: A retrospective study. Pediatric Pulmonology, 58(10), 2815-2822. https://doi.org/10.1002/ppul.26593 PMid:37431970

7. Li, M., Wei, X., Zhang, S.-S., Li, S., Chen, S.-H., Shi, S.-J., Zhou, S.-H., Sun, D.-Q., Zhao, Q., & Xu, Y. (2023). Recognition of refractory Mycoplasma pneumoniae pneumonia among Myocoplasma pneumoniae pneumonia in hospitalized children: development and validation of a predictive nomogram model. BMC Pulmonary Medicine, 23. https://doi.org/10.1186/s12890-023-02684-1 PMid:37817172 PMCid:PMC10566172
8. Li, L., Guo, R., Zou, Y., Wang, X., Wang, Y., Zhang, S., Wang, H., Jin, X., & Zhang, N. (2024). Construction and Validation of a Nomogram Model to Predict the Severity of Mycoplasma pneumoniae Pneumonia in Children. Journal of Inflammation Research, 17, 1183-1191. https://doi.org/10.2147/JIR.S447569 PMid:38410419 PMCid:PMC10895981
9. Zhang, Y. Y., Dai, L. M., Zhou, Y. L., Yang, D. H., Tang, L. F., & Chen, Z. M. (2019). Zhonghua er ke za zhi = Chinese journal of pediatrics, 57(8), 625-630.
10. Chen, Q., Hu, T., Wu, L., & Chen, L. (2024). Clinical Features and Biomarkers for Early Prediction of Refractory Mycoplasma Pneumoniae Pneumonia in Children. Emergency medicine international, 2024, 9328177. https://doi.org/10.1155/2024/9328177 PMid:38222094 PMCid:PMC10787049
11. Li, M., Chen, Y., Li, H., Yang, D., Zhou, Y., Chen, Z., & Zhang, Y. (2021). Serum CXCL10/IP-10 may be a potential biomarker for severe Mycoplasma pneumoniae pneumonia in children. BMC infectious diseases, 21(1), 909. https://doi.org/10.1186/s12879-021-06632-4 PMid:34481469 PMCid:PMC8418284
12. Wang, L. P., Hu, Z. H., Jiang, J. S., & Jin, J. (2024). Serum inflammatory markers in children with Mycoplasma pneumoniae pneumonia and their predictive value for mycoplasma severity. World journal of clinical cases, 12(22), 4940-4946. https://doi.org/10.12998/wjcc.v12.i22.4940 PMid:39109035 PMCid:PMC11238786
13. World Health Organization Vaccine Trials Investigators' Group. (2001). Standardization of interpretation of chest radiographs for the diagnosis of pneumonia in children (WHO/V&B/01.35). Geneva: World Health Organization. Retrieved from https://who-cres.mcri.edu.au/media/1315/who-vaccine-trials-group-cxr-stand-doc.pdf
14. Zhou, Y., Hu, M., Ye, B., Chen, Z., & Zhang, Y. (2020). Early prediction of necrotizing pneumonia from mycoplasma pneumoniae pneumonia with large pulmonary lesions in children. Scientific reports, 10(1), 19061. https://doi.org/10.1038/s41598-020-76083-5 PMid:33149220 PMCid:PMC7643079
15. Ardila, S. M., Weeks, H. M., Dahmer, M. K., Kaciroti, N., Quasney, M., Sapru, A., Curley, M. A. Q., Flori, H. R., & Biomarkers in Children with Acute Lung Injury (BALI) and Randomized Evaluation for Sedation Titration for Respiratory Failure (RESTORE) Study Investigators and Pediatric Acute Lung Injury and Sepsis Investigators (PALISI) Network (2023). A Targeted Analysis of Serial Cytokine Measures and Nonpulmonary Organ System Failure in Children With Acute Respiratory Failure: Individual Measures and Trajectories Over Time. Pediatric critical care medicine: a journal of the Society of Critical Care Medicine and the World Federation of Pediatric Intensive and Critical Care Societies, 24(9), 727-737. https://doi.org/10.1097/PCC.0000000000003286 PMid:37195096 PMCid:PMC10524322
16. Collins, G. S., Reitsma, J. B., Altman, D. G., & Moons, K. G. (2015). Transparent reporting of a multivariable prediction model for individual prognosis or diagnosis (TRIPOD): the TRIPOD statement. BMJ (Clinical research ed.), 350, g7594. https://doi.org/10.1161/CIRCULATIONAHA.114.014508 PMCid:PMC4297220
17. World Health Organization Vaccine Trials Investigators' Group. Standardization of interpretation of chest radiographs for the diagnosis of pneumonia in children. 2001. https://who-cres.mcri.edu.au/media/1315/who-vaccine-trials-group-cxr-stand-doc.pdf
18. American College of Radiology. ACR Appropriateness Criteria®: Pneumonia in the immunocompetent child. 2019. https://acsearch.acr.org/docs/3102387/Narrative/
19. Vickers, A. J., & Elkin, E. B. (2006). Decision curve analysis: a novel method for evaluating prediction models. Medical decision making : an international journal of the Society for Medical Decision Making, 26(6), 565-574. https://doi.org/10.1177/0272989X06295361 PMid:17099194 PMCid:PMC2577036
20. Fernandes, C. D., Arriaga, M. B., Costa, M. C. M., Costa, M. C. M., Costa, M. H. M., Vinhaes, C. L., Silveira-Mattos, P. S., Fukutani, K. F., & Andrade, B. B. (2019). Host Inflammatory Biomarkers of Disease Severity in Pediatric Community-Acquired Pneumonia: A Systematic Review and Meta-analysis. Open forum infectious diseases, 6(12), ofz520. https://doi.org/10.1093/ofid/ofz520 PMid:31867405 PMCid:PMC6917028
21. Yang, M., Meng, F., Gao, M., Cheng, G., & Wang, X. (2019). Cytokine signatures associate with disease severity in children with Mycoplasma pneumoniae pneumonia. Scientific reports, 9(1), 17853. https://doi.org/10.1038/s41598-019-54313-9 PMid:31780733 PMCid:PMC6882793
22. Ding, S., Wang, X., Chen, W., Fang, Y., Liu, B., Liu, Y., Fei, G., & Wang, L. (2016). Decreased Interleukin-10 Responses in Children with Severe Mycoplasma pneumoniae Pneumonia. PloS one, 11(1), e0146397. https://doi.org/10.1371/journal.pone.0146397 PMid:26751073 PMCid:PMC4708986
23. Li, P., Liu, J., & Liu, J. (2022). Procalcitonin-guided antibiotic therapy for pediatrics with infective disease: A updated meta-analyses and trial sequential analysis. Frontiers in cellular and infection microbiology, 12, 915463. https://doi.org/10.3389/fcimb.2022.915463 PMid:36211950 PMCid:PMC9532766
24. Chen, Y., Li, L., Wang, C., Zhang, Y., & Zhou, Y. (2023). Necrotizing Pneumonia in Children: Early Recognition and Management. Journal of clinical medicine, 12(6), 2256. https://doi.org/10.3390/jcm12062256 PMid:36983257 PMCid:PMC10051935
25. de Jager, W., Bourcier, K., Rijkers, G. T., Prakken, B. J., & Seyfert-Margolis, V. (2009). Prerequisites for cytokine measurements in clinical trials with multiplex immunoassays. BMC immunology, 10, 52. https://doi.org/10.1186/1471-2172-10-52 PMid:19785746 PMCid:PMC2761376
26. Firth, D. (1993). Bias reduction of maximum likelihood estimates. Biometrika, 80(1), 27-38. https://doi.org/10.1093/biomet/80.1.27
27. Efron, B., & Tibshirani, R. (1997). Improvements on cross-validation: The .632+ bootstrap method. Journal of the American Statistical Association, 92(438), 548-560. https://doi.org/10.1080/01621459.1997.10474007
28. Kim, K., Jung, S., Kim, M., Park, S., Yang, H. J., & Lee, E. (2022). Global Trends in the Proportion of Macrolide-Resistant Mycoplasma pneumoniae Infections: A Systematic Review and Meta-analysis. JAMA network open, 5(7), e2220949. https://doi.org/10.1001/jamanetworkopen.2022.20949 PMid:35816304 PMCid:PMC9274321
29. Centers for Disease Control and Prevention. (2024). Clinical care of Mycoplasma pneumoniae infection. U.S. Department of Health & Human Services. https://www.cdc.gov/mycoplasma/hcp/clinical-care/index.html